Available online at www.sciencedirect.com
ScienceDirect
Trans. Nonferrous Met. Soc. China 26(2016) 310−318
Transactions of Nonferrous Metals Society of China
www.tnmsc.cn

Electrodeposition of As−Sb alloy from high arsenic-containing solutions

Hua-zhen CAO, Yang ZHONG, Lian-kui WU, Yu-feng ZHANG, Guo-qu ZHENG

College of Materials Science and Engineering, Zhejiang University of Technology, Hangzhou 310014, China

Received 26 January 2015; accepted 8 September 2015

Abstract: As−Sb alloy was electrodeposited from high arsenic-containing solutions. The influences of current density, Sb^{3+} concentration, reaction temperature and HCl concentration on the electrolyte composition, cell voltage and current efficiency were investigated. The surface morphology, composition and structure of the deposits were analyzed by scanning electron microscopy (SEM), inductively coupled plasma mass spectrometry (ICP-MS) and X-ray diffraction (XRD), respectively. The results show that the prepared As−Sb alloy shows an amorphous structure under all conditions. Under the optimized condition, i.e., 10 g/L As^{3+}, 2 g/L Sb^{3+}, 4 mol/L HCl, current density of 4 mA/cm^2 and temperature of 20 °C, desired As−Sb alloy with a composition of 70.26% As and 29.74% Sb (mass fraction) is obtained. What is more, the current efficiency is as high as 94.74% and high arsenic removal rate is achieved under this condition.

Key words: arsenic-containing solution; hydrochloric system; electrodeposition; As−Sb alloy

1 Introduction

Until now, many scientists have exploited various technologies and materials to remove arsenic efficiently, such as chemical precipitation [1], adsorption [2], ion exchange [3], membrane separation [4], biological removal [5] and electrocoagulation [6]. By these methods, a large number of arsenic-bearing compounds were produced, most of which cannot be reused and had to be accumulated perennially, causing secondary pollution easily. Therefore, the recovery processing of the arsenic-containing waste becomes the research direction in this field, that is to say, not only toxic arsenic pollution should be eliminated, but also useful arsenic resource can be obtained simultaneously. The fabrication of nontoxic elementary arsenic from high arsenic-containing solutions by electrochemical deposition is one of the efficient methods and has attracted most research interest. However, toxic AsH_3 will be produced during the electrodeposition process [7,8] and the nonconductive arsenic film causes the current efficiency to decrease remarkably [9], which restricts the application of this method.

As−Sb alloy and As−Sb-based alloy have broad application perspective in many areas due to the excellent semiconductor property [10,11], photoelectric property [12], thermoelectric property [13,14] and electromagnetic property [15]. MUSIANI et al [16] prepared As−Sb alloy by electrodeposition in citric acid solutions containing As_2O_3 and $SbCl_3$ and discussed the relationship between the electric-conductivity of alloy and the mole ratio of As to Sb in alloy, which depended on the concentrations of arsenic and antimony in electrolyte. Besides, the structure of deposits [17] and the kinetic model of electrodeposition process [18] were analyzed. Our previous studies [19,20] found that the nucleation process of As−Sb alloy on glassy carbon electrode follows the three-dimensional growth mechanism under diffusion limitations, and the toxic AsH_3 can be efficiently inhibited during the electrodeposition by the addition of Sb^{3+} into arsenic-containing solution.

This study focuses on the arsenic-containing hydrochloric acid solution produced from the leaching and the continuous distillation process of antimony-rich lead anode [21,22], for which electrodeposition method was adopted to extract arsenic and get As−Sb alloy. The influences of HCl concentration, Sb^{3+} concentration, current density and reaction temperature on the electrolyte composition, cell voltage, current efficiency as well as the composition of the deposit were investigated. It is expected that by doing this, the toxic arsenic contaminants can be eliminated and the recycle

Foundation item: Project (51374185) supported by the National Natural Science Foundation of China
Corresponding author: Guo-qu ZHENG; Tel: +86-571-88320429; E-mail: zhenggq@zjut.edu.cn
DOI: 10.1016/S1003-6326(16)64120-1

of arsenic resource and hydrochloric acid solution can be realized.

2 Experimental

2.1 Raw material

Arsenic-containing hydrochloric acid solution and crystal antimony trichloride were derived from the chloridizing leaching process of lead anode slime containing arsenic and antimony, which were purified by double distillation before use. Various solutions with different contents of As^{3+}, Sb^{3+} and hydrochloric acid were prepared from the purified $AsCl_3$ hydrochloric acid solutions and crystal $SbCl_3$.

2.2 Electrodeposition

The electrodeposition of As−Sb alloy was carried out in a sealed cell with a volume of 290 mL under certain current density. Copper plate (30 mm × 60 mm × 2 mm) and graphite were used as cathode and anode, respectively. High purity nitrogen was kept bubbling to drive away the generated AsH_3 and SbH_3 on the cathode, which was then adsorbed with 4 mol/L HNO_3 solution. The current efficiency was calculated according to Eq. (1):

$$\eta = \frac{3F\left(\frac{m_{As}}{M_{As}} + \frac{m_{Sb}}{M_{Sb}}\right)}{It} \quad (1)$$

where m_{As} and m_{Sb} (g) are the mass of arsenic and antimony in deposits, respectively, M_{As} and M_{Sb} (g/mol) stand for the relative mole mass of arsenic and antimony, respectively, F (C/mol) is the Faraday constant, I (A) and t (s) are the applied current and time, respectively.

2.3 Characterization

Sb^{3+} was titrated by ceric sulfate and As^{3+} was titrated by potassium bromate in hydrochloric acid medium with methylene blue−methyl orange as indicator. Inductively coupled plasma optical emission spectrometer (Leeman Prodigy) was used to analyze the trace amount of Sb^{3+} and As^{3+}. The structure and surface morphologies of deposits were characterized by X-ray diffraction (XRD, RIGAKU D/Max 2550 PC) and scanning electron microscopy (SEM, VEGA3), respectively. The cathodic deposits were dissolved with 6 mol/L HCl and H_2O_2, and then inductively coupled plasma mass spectrometry (ICP-MS) was applied to analyzing the amount of arsenic and antimony.

3 Results and discussion

3.1 Effects of current density on electrodeposition of As−Sb alloy

The concentration variation of each ion in electrolyte during the electrodeposition under different current densities are shown in Fig. 1. It is observed that the As^{3+} and Sb^{3+} concentrations keep declining while those of As^{5+} and Sb^{5+} increase as the electrodeposition progresses. As^{5+} and Sb^{5+} generate from the oxidation reaction on the graphite anode. The decrease of As^{3+} and Sb^{3+} concentrations is mainly due to the cathodic reduction to form As−Sb alloy and the anodic oxidization to produce As^{5+} and Sb^{5+}. Besides, trace amount of As^{3+} and Sb^{3+} may be reduced to form AsH_3 and SbH_3.

From Fig. 1, the concentrations of As^{3+} and Sb^{3+} change slowly at the current density of 1 mA/cm^2, indicating low removal efficiency. With the current density increasing to 4 mA/cm^2, the concentration of As^{3+} declines rapidly in the initial 90 min, after which the rate slows down, while the concentration of Sb^{3+} decreases in a fast rate during the whole electrodeposition process. Simultaneously, there is a fast increase of concentrations of As^{5+} and Sb^{5+}. The accumulation of these pentavalent ions to a certain amount will play a negative role in the cathodic deposits, i.e., the black granules mainly composed of oxides are produced on the surface of deposits. So, how to keep a stable and slow increase rate for the concentrations of As^{5+} and Sb^{5+} is one of the critical factors to obtain high-quality electrodeposits.

The mass and compositions of the electrodeposited film as well as the current efficiencies at different current densities are displayed in Table 1. It is shown that the cathodic current efficiency at 4 mA/cm^2 is 96.39%. That is to say, 3.61% actual electricity may be contributed to the generation of AsH_3 and SbH_3 at the cathode. This result is consistent with the previous research [19], in which As−Sb alloy was electrodeposited from a low arsenic-containing solution and the actual electricity used for the AsH_3 evolution is only 2.12%. Furthermore, the composition of electrodeposits changes with the applied current density. When the current density increases from 1 to 4 mA/cm^2, the mass fraction of arsenic in the electrodeposits reduces from 57.14% to 33.11%, suggesting that the current density plays an important role in the composition of the electrodeposits. However, the amount of deposits is abundant at 4 mA/cm^2, in this case, the mass of As in deposits reaches 0.1802 g, more than that obtained at 1 mA/cm^2, which means higher removal rate of As^{3+} at 4 mA/cm^2.

The prepared As−Sb alloy presents a typical metallic luster. The surface is uniform and even with silver-white appearance. Figure 2 shows the XRD patterns of electrodeposits at different current densities. Two broad peaks appear in 2θ ranges of 21°−40° and 46°−58°, which are similar to the XRD patterns of

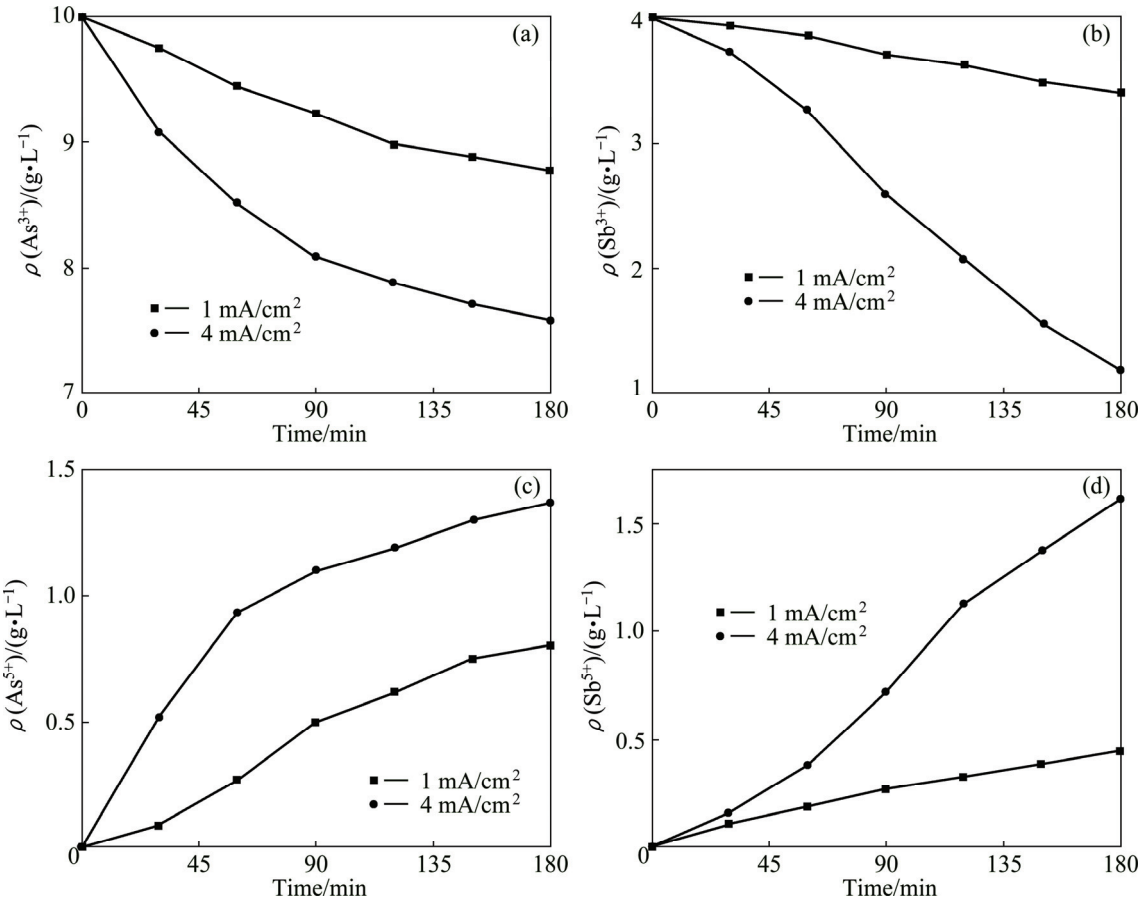

Fig. 1 Variation of concentrations of As^{3+} (a), Sb^{3+} (b), As^{5+} (c) and Sb^{5+} (d) in electrolyte during electrodeposition at current densities of 1 and 4 mA/cm^2 (20 °C, HCl concentration of 3 mol/L, As^{3+} concentration of 10 g/L, Sb^{3+} concentration of 4 g/L)

Table 1 Mass and compositions of electrodeposits as well as current efficiencies at different current densities

current density/ (mA·cm^{-2})	Mass of deposits/g	Mass of As in deposits/g	Mass fraction of As/%	Mass fraction of Sb/%	Current efficiency/%
1	0.1321	0.07548	57.14	42.86	98.20
4	0.5441	0.1802	33.11	66.89	96.39

electrodeposited As [23]. It is observed that even when the content of antimony in alloy reaches 66.89%, there are no typical antimony diffraction peaks. Therefore, the electrodeposits have an amorphous structure.

The evolution of the cell voltage during the electrodeposition at different current densities is shown in Fig. 3. When the current density is 1 mA/cm^2, the cell voltage is 1.0 V at the initial 60 min, then it increases to 1.1 V and remains unchanged. Under the condition of 4 mA/cm^2, the cell voltage is 1.3 V at the initial 30 min, then, it gradually increases to 1.6 V. This phenomenon indicates good electrical conductive property of the electrodeposits, even the Sb^{3+} concentration reduces to ~1 g/L after electrodeposition for 180 min.

It is obvious that 4 mA/cm^2 is an appropriate current density due to good quality of electrodeposits, high removal rate of As^{3+} and current efficiency.

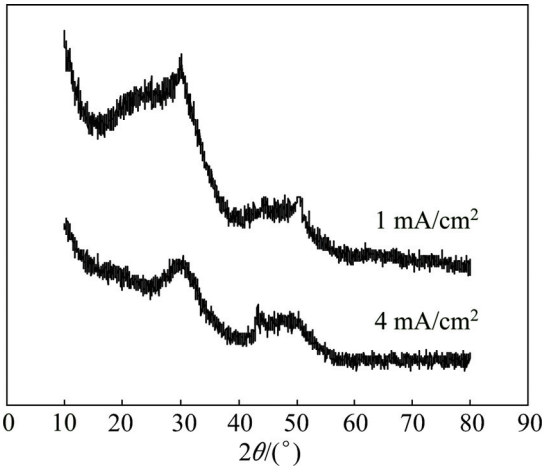

Fig. 2 XRD patterns of electrodeposits at different current densities (20 °C, HCl concentration of 3 mol/L, As^{3+} concentration of 10 g/L, Sb^{3+} concentration of 4 g/L)

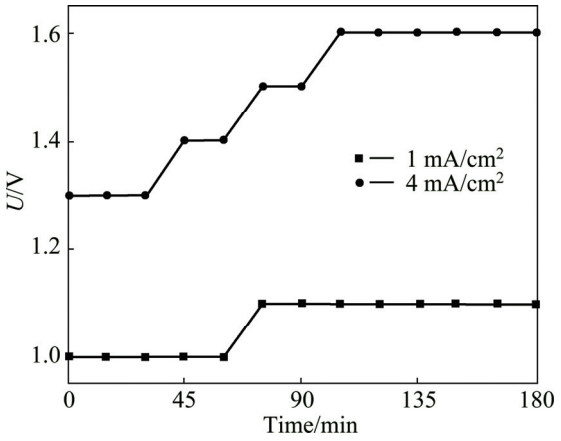

Fig. 3 Variation of cell voltage during electrodeposition at different current densities (20 °C, HCl concentration of 3 mol/L, As^{3+} concentration of 10 g/L and Sb^{3+} concentration of 4 g/L)

3.2 Effect of Sb^{3+} concentration on electrodeposition of As−Sb alloy

Figure 4 shows the concentration variation of each ion in electrolyte during the electrodeposition under different initial Sb^{3+} concentrations. It is found that the initial Sb^{3+} concentration has little influence on the variation of As^{3+} and As^{5+} concentrations, but there is an obvious acceleration in the decrease of Sb^{3+} concentration and the increase of Sb^{5+} concentration under the initial Sb^{3+} concentration of 4 g/L. These results indicate that high initial Sb^{3+} concentration is not beneficial to the electrodeposition of As−Sb alloy since large number of pentavalent ions generate in this case and deteriorate the quality of electrodeposits.

Table 2 shows the mass and compositions of electrodeposits as well as the current efficiencies under different initial Sb^{3+} concentrations. It is obvious that more products are obtained at the initial Sb^{3+} concentration of 4 g/L, while the content of As in deposits is only 33.11%, which is as high as 67.13% at the initial Sb^{3+} concentration of 1 g/L. Therefore, the composition of alloy can be controllable by adjusting the initial Sb^{3+} concentration.

Although the mass of As in deposits is the most at the initial Sb^{3+} concentration of 1 g/L, the corresponding current efficiency is only 88.49%, which means that the side reaction is obvious. The low current efficiency at the initial Sb^{3+} concentration of 1 g/L maybe results from the

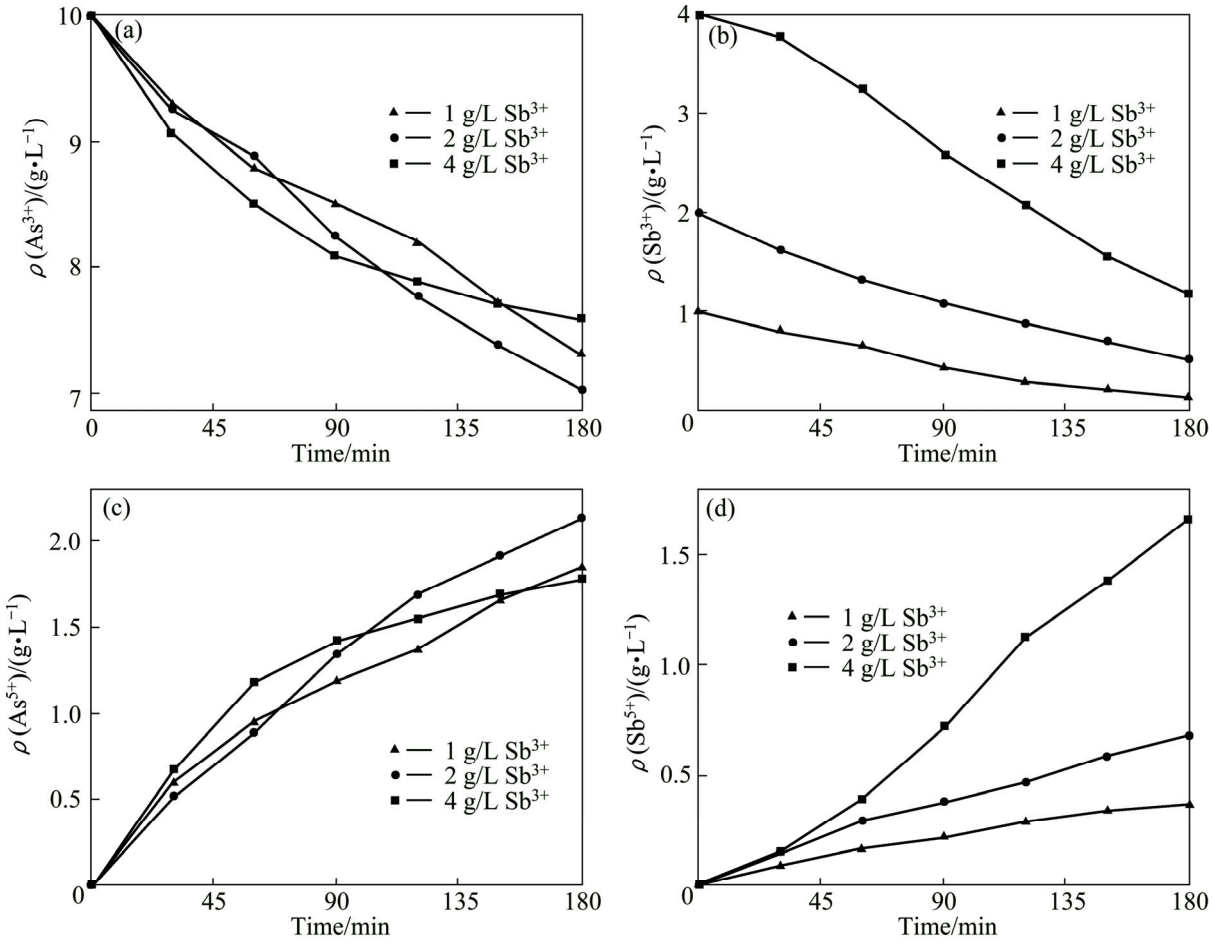

Fig. 4 Variation of concentrations of As^{3+} (a), Sb^{3+} (b), As^{5+} (c) and Sb^{5+} (d) in electrolyte during electrodeposition with initial Sb^{3+} concentrations of 1, 2 and 4 g/L (20 °C, HCl concentration of 3 mol/L, As^{3+} concentration of 10 g/L, current density of 4 mA/cm^2)

Table 2 Mass and compositions of electrodeposits as well as current efficiencies under different initial Sb^{3+} concentrations

$\rho(Sb^{3+})$/ ($g\cdot L^{-1}$)	Mass of deposits/g	Mass of As in deposits/g	Mass fraction of As/%	Mass fraction of Sb/%	Current efficiency/%
4	0.5441	0.1802	33.11	66.89	96.39
2	0.5188	0.2322	44.77	55.23	97.46
1	0.4247	0.2851	67.13	32.87	88.49

long time electrodeposition, causing the Sb^{3+} concentration in solution decrease to a very low level at which the electrodeposits are mainly composed of nonconductive As. So, the electrodeposition process is hindered and more toxic gas may be released under this condition.

The variation of cell voltage under different initial Sb^{3+} concentrations is shown in Fig. 5. For the initial Sb^{3+} concentration of 1 g/L, the cell voltage rises fast accompanied with large number of gas evolution and reaches 3.3 V after deposition for 180 min, indicating a poor electrodeposition layer. When the initial Sb^{3+} concentration is over 2 g/L, the cell voltage increases slowly not exceeding 1.8 V, and the As−Sb deposits exhibit a macro-smooth surface with silver-white metallic luster. Compared comprehensively, the initial Sb^{3+} concentration of 2 g/L is a suitable deposition condition due to the excellent conductivity and appearance of electrodeposits, high removal rate of As^{3+} and current efficiency.

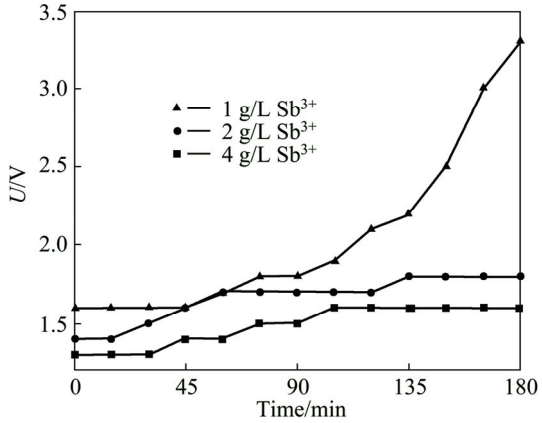

Fig. 5 Variation of cell voltage during electrodeposition under different initial Sb^{3+} concentrations (20 °C, HCl concentration of 3 mol/L, As^{3+} concentration of 10 g/L, current density of 4 mA/cm^2)

3.3 Effect of reaction temperature on electrodeposition of As−Sb alloy

Figure 6 shows the concentration variation of each ion in the electrolyte during electrodeposition at different temperatures. It is observed that temperature has a small influence on the variation of As^{3+}, Sb^{3+}, As^{5+} and Sb^{5+} concentrations. The mass and compositions of the electrodeposits as well as the current efficiencies at different temperature are shown in Table 3.

The content of arsenic in the deposit is about 45% at 10 and 20 °C, slightly below that prepared at 30 °C. The current efficiency at 20 °C reaches 97.46%, higher than those at other temperatures. The decrease of current efficiency at 30 °C may be caused by the increased side reaction, such as gas evolution.

Figure 7 shows the variation of cell voltage during the electrodeposition at different temperatures. In general, the cell voltage decreases as the temperature increases. Specifically, the cell voltages are very close at 10 and 20 °C and the variation of the cell voltages are similar at all temperatures. However, the surface of As−Sb deposits prepared at 30 °C becomes rough. Therefore, 20 °C is the appropriate reaction temperature for the electrodeposition due to the high current efficiency and good quality of electrodeposits.

3.4 Effect of HCl concentration on electrodeposition of As−Sb alloy

Figure 8 shows the concentration variation of each ion in electrolyte during the electrodeposition under different HCl concentrations. It can be seen that the HCl concentration has a great influence on the variation of As^{3+}, Sb^{3+}, As^{5+} and Sb^{5+} concentrations. For the case of 2 mol/L HCl, the concentrations of As^{3+} and As^{5+} change slowly, whereas the Sb^{3+} concentration reduces remarkably and there is a rapid increase of Sb^{5+} concentration, leading to an adverse effect on the quality of electrodeposits. The surface of deposits is covered with large number of black particles after deposition for 180 min. Moreover, there appear obvious micro-cracks on the surface, as shown in Fig. 9(a). When the HCl concentration increases to 3 mol/L, a similar result as that in solution of 2 mol/L HCl is observed. It can be seen from Fig. 9(b) that there still exists microvoid on the surface although the surface becomes smoother. When the HCl concentration is 4 mol/L, the concentration of As^{3+} decreases rapidly while those of As^{5+} and Sb^{5+} increase gently. In this case, the deposits are compact and smooth without any cracks on the surface, as shown in Fig. 9(c).

The mass and compositions of electrodeposits as well as the current efficiencies obtained at different HCl concentrations are displayed in Table 4. The arsenic content in electrodeposits increases as the HCl

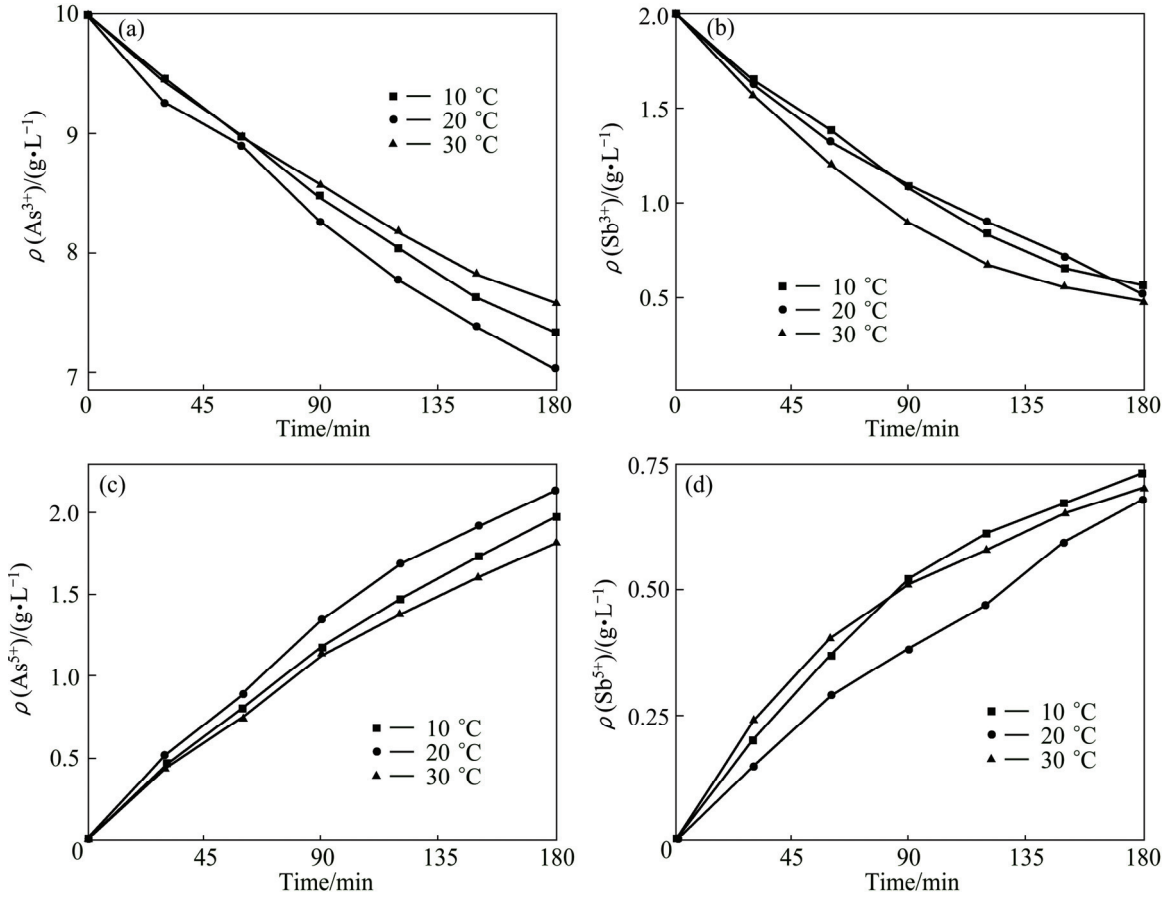

Fig. 6 Variation of concentrations of As^{3+} (a), Sb^{3+} (b), As^{5+} (c) and Sb^{5+} (d) in electrolyte during electrodeposition at 10, 20 and 30 °C (HCl concentration of 3 mol/L, As^{3+} concentration of 10 g/L, current density of 4 mA/cm^2)

Table 3 Mass and compositions of electrodeposited films as well as current efficiencies at different temperatures

Temperature/ °C	Mass of deposits/g	Mass of As in deposits/g	Mass fraction of As/%	Mass fraction of Sb/%	Current efficiency/%
10	0.4945	0.2253	45.56	54.44	93.25
20	0.5188	0.2322	44.77	55.23	97.46
30	0.4839	0.2486	51.37	48.63	93.83

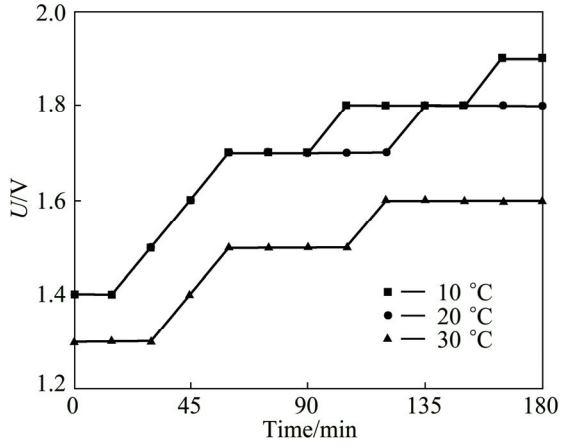

Fig. 7 Variation of cell voltage during electrodeposition at different temperatures (HCl concentration of 3 mol/L, As^{3+} concentration of 10 g/L, current density of 4 mA/cm^2)

concentration increases. In the solution containing 2 mol/L HCl, the arsenic content is only 34.71%, which increases to 70.26% in the solution with 4 mol/L HCl. This indicates that the HCl concentration has a great influence on the composition of eletrodeposits. Besides, when the HCl concentration is above 3 mol/L, the corresponding current efficiency exceeds 94%, much higher than that obtained in the solution with 2 mol/L HCl.

The variation of cell voltage during the electrodeposition under different HCl concentrations is shown in Fig. 10. It is found that the cell voltage decreases as the HCl concentration increases. In solutions with 3 and 4 mol/L HCl, the cell voltage is below 1.8 V during the whole deposition process. However, for the case of 2 mol/L HCl, the cell voltage

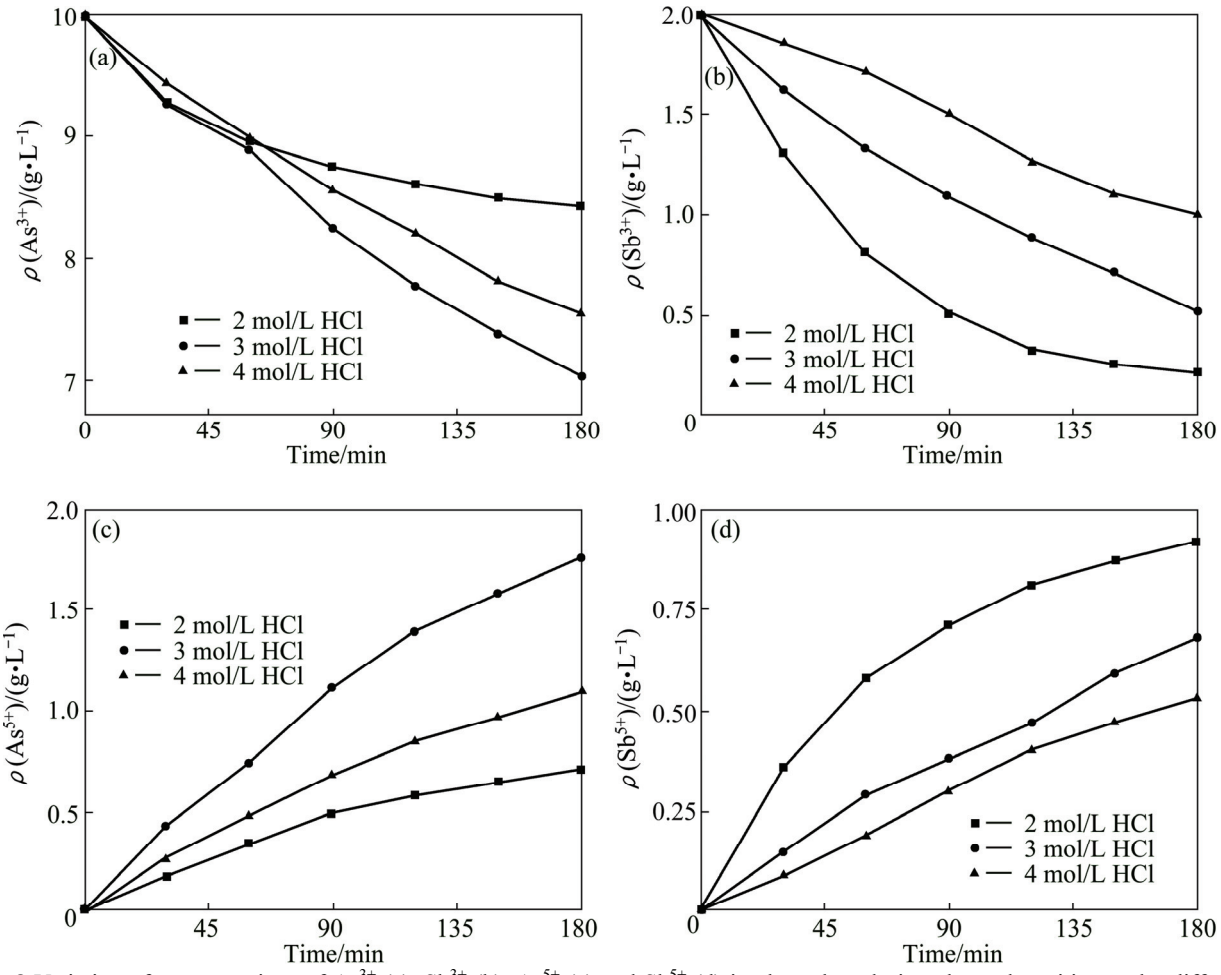

Fig. 8 Variation of concentrations of As^{3+} (a), Sb^{3+} (b), As^{5+} (c) and Sb^{5+} (d) in electrolyte during electrodeposition under different HCl concentrations (20 °C, As^{3+} concentration of 10 g/L, Sb^{3+} concentration of 2 g/L, current density of 4 mA/cm^2)

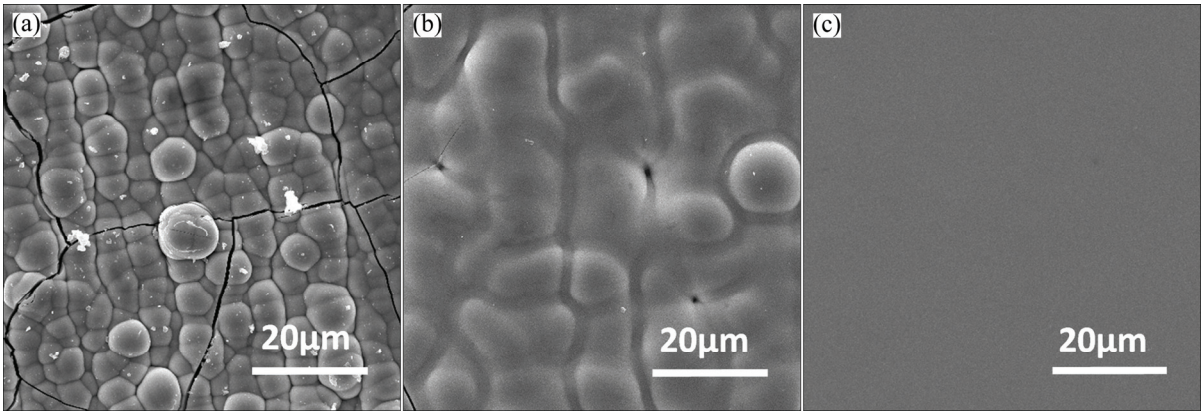

Fig. 9 SEM images of deposits prepared in solutions containing 2 mol/L HCl (a), 3 mol/L HCl (b) and 4 mol/L HCl (c) (20 °C, As^{3+} concentration of 10 g/L, Sb^{3+} concentration of 2 g/L, current density of 4 mA/cm^2)

Table 4 Mass and compositions of electrodeposits as well as current efficiencies under different HCl concentrations

c(HCl)/ (mol·L^{-1})	Mass of deposits/g	Mass of As in deposits/g	Mass fraction of As/%	Mass fraction of Sb/%	Current efficiency/ %
2	0.3820	0.1326	34.71	65.29	68.23
3	0.5188	0.2323	44.77	55.23	97.46
4	0.4485	0.3151	70.26	29.74	94.74

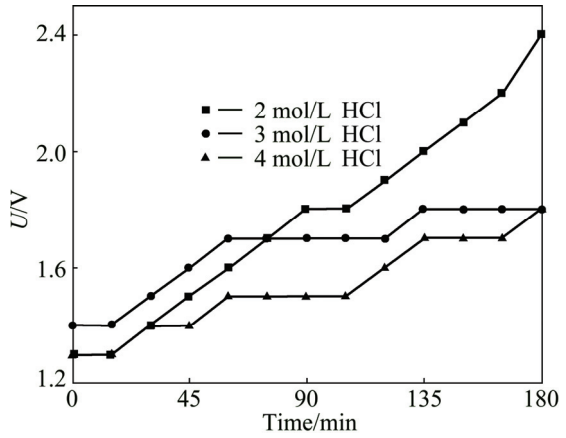

Fig. 10 Variation of cell voltage during electrodeposition under different HCl concentrations (20 °C, As^{3+} concentration of 10 g/L, Sb^{3+} concentration of 2 g/L, current density of 4 mA/cm^2)

increases rapidly and reaches 2.4 V after 180 min, and a large amount of gas generates simultaneously on the cathode. Therefore, 4 mol/L HCl is the suitable condition for the electrodeposition of As−Sb alloy considering the high arsenic removal rate and current efficiency.

4 Conclusions

1) Compact As−Sb alloy with silver-white metallic luster was successfully fabricated by electrodeposition from HCl solution containing As^{3+} and appropriate amount of Sb^{3+}.

2) The current density, Sb^{3+} concentration, temperature and HCl concentration have a great influence on the composition of electrodeposits. The prepared As−Sb alloy shows an amorphous structure under the studied conditions.

3) As−Sb alloy with good quality can be obtained in solution with 10 g/L As^{3+}, 2 g/L Sb^{3+} and 4 mol/L HCl at current density of 4 mA/cm^2 and 20 °C. Under this condition, the deposits are composed of 70.26% As and 29.74% Sb, and the current efficiency and arsenic removal rate are high.

References

[1] YI Yu, SHI Jing, TIAN Qing-hua, GUO Xue-yi. Arsenic removal from high-arsenic dust by NaOH−Na_2S alkaline leaching [J]. The Chinese Journal of Nonferrous Metals, 2015, 25(3): 806−814. (in Chinese)

[2] GILES D E, MOHAPATRA M, ISSA T B, SINGH P. Iron and aluminum based adsorption strategies for removing arsenic from water [J]. Journal of Environmental Management, 2011, 92(12): 3011−3022.

[3] SHAO Wen-jing, LI Xiao-min, CAO Qi-lin, LUO Fang, LI Jian-mei, DU Yang-yang. Adsorption of arsenate and arsenite anions from aqueous medium by using metal(III)-loaded amberlite resins [J]. Hydrometallurgy, 2008, 91(1): 138−143.

[4] NGUYEN C M, BANG S, CHO J, KIM K W. Performance and mechanism of arsenic removal from water by a nanofiltration membrane [J]. Desalination, 2009, 245(1−3): 82−94.

[5] SU Shi-ming, ZENG Xi-bai, BAI Ling-yu, LI Lian-fang, DUAN Ran. Arsenic biotransformation by arsenic-resistant fungi *Trichoderma asperellum* SM-12F1, *Penicillium janthinellum* SM-12F4, and *Fusarium oxysporum* CZ-8F1 [J]. Science of the Total Environment, 2011, 409(23): 5057−5062.

[6] BALASUBRAMANIAN N, KOJIMA T, SRINIVASAKANAN C. Arsenic removal through electrocoagulation: Kinetic and statistical modeling [J]. Chemical Engineering Journal, 2009, 155(1−2): 76−82.

[7] BEJAN D, BUNCE N J. Electrochemical reduction of As(III) and As(V) in acidic and basic solutions [J]. Journal of Applied Electrochemistry, 2003, 33(6): 483−489.

[8] WEI Z, SOMASUNDARAN P. Cyclic voltammetric study of arsenic reduction and oxidation in hydrochloric acid using a Pt RDE [J]. Journal of Applied Electrochemistry, 2004, 34(2): 241−244.

[9] MENZIEST I A, OWEN L W. The electrodeposition of arsenic from aqueous and non-aqueous solutions [J]. Electrochimica Acta, 1966, 11: 251−255.

[10] HE J, REYNER C J, LIANG B L, NUNNA K, HUFFAKER D L. Band alignment tailoring of $InAs_{1-x}Sb_x$/GaAs quantum dots: Control of type I to type II transition [J]. Nano Lett, 2010, 10(8): 3052−3056.

[11] BOUARISSA N, BACHIRI R, CHARIFI Z. Electronic properties of $Al_xGa_{1-x}As_ySb_{1-y}$ alloys lattice-matched to InAs [J]. Physica Status Solidi, 2001, 226(2): 293−304.

[12] BELABBES A, ZAOUI A, FERHAT M. Alloying effect in the III-As−Sb ternary systems [J]. Materials Science and Engineering B, 2007, 137(1−3): 210−212.

[13] MUNTYANUF M, QUANTUM A. Oscillations of magnetoresistance and thermomagnetic power and the fermi surface of AsSb alloys [J]. Physica Status Solidi, 1986, 136: 749−756.

[14] GITSU D V, GOLBANI M, MAKEICHIKA I, MUNTYANUF M, ONU M I. The thermopower and the thermomagnetic power in arsenic−antimony alloys at low temperature [J]. Physica Status Solidi, 1980, 100: 401−406.

[15] SHAKHTINSKAYAM I, TOMTIEVD S. Galvanomagnetic properties and band structure of the Bi−Sb−As system [J]. Physica Status Solidi, 1971, 46: 425−428.

[16] MUSIANI M M, PAOLUCCI F, GUERRIERO P. Electrodeposition of As−Sb alloys [J]. Journal of Electroanalytical Chemistry, 1992, 332(1−2): 113−126.

[17] BERTONCELLO R, GLISENTI A, GRANOZZI G, MUSIANI M M. Angle-resolved X-ray photoelectron spectroscopy contribution to elucidation of the mechanism of cathodic deposition of As−Sb alloys [J]. Journal of Electroanalytical Chemistry, 1994, 374(1−2): 37−43.

[18] MUSIANI M M, PAGURA C. Kinetic model of the cathodic deposition of As−Sb alloys [J]. Journal of Electroanalytical Chemistry, 1993, 352(1−2): 197−212.

[19] CAO Hua-zhen, WAN Qiang-bo, SHAN Hai-peng, RUAN Hui-min, ZHENG Guo-qu. Preparation of arsenic−antimony alloy by electrodeposition inhydrochloric acid system [J]. The Chinese Journal of Nonferrous Metals, 2012, 22(12): 3548−3554. (in Chinese)

[20] CAO Hua-zhen, SHAN Hai-peng, RUAN Hui-min, ZHENG Guo-qu. A study on the evolution of arsine during arsenic electrodeposition: The influence of ammonium citrate [J]. Electrochemistry Communications, 2012, 23: 44−47.

[21] CAO Hua-zhen, CHEN Jin-zhong, YUAN Hai-jun, ZHENG Guo-qu. Preparation of pure $SbCl_3$ from lead anode slime bearing high antimony and low silver [J]. Transactions of Nonferrous Metals

Society of China, 2010, 20(12): 2379−2403.
[22] CHEN Jin-zhon, CAO Hua-zheng, LI Bo, ZHENG Guo-qu. Thermodynamic analysis of separating lead and antimony in chloride system [J]. Transactions of Nonferrous Metals Society of China, 2009, 19(3): 730−734.
[23] KOZLOV V M, BOZZINI B, BICELLI L P. Preparation of InAs by annealing of two-layer In−As electrodeposits [J]. Journal of Alloys and Compounds, 2004, 366(1−2): 152−160.

高浓度砷溶液中电沉积 As−Sb 合金

曹华珍，钟 杨，伍廉奎，张煜峰，郑国渠

浙江工业大学 材料科学与工程学院，杭州 310014

摘 要：在高浓度砷溶液中采用电沉积法制备 As−Sb 合金，考察电解液中电流密度、Sb^{3+}浓度、反应温度和盐酸浓度对电沉积过程中电解液成分、槽电压和电流效率的影响，并采用扫描电镜(SEM)、电感藕合等离子体质谱(ICP-MS)和 X 射线衍射(XRD)分别对沉积物的表面形貌、成分和结构进行分析。结果表明：在所研究的工艺条件下制备的 As−Sb 合金沉积层均为非晶结构。最优工艺如下：As^{3+}浓度为 10 g/L，Sb^{3+}浓度为 2 g/L，盐酸浓度为 4 mol/L，电流密度为 4 mA/cm^2，温度为 20 °C，在此条件下电流效率达到 94.74%，沉积层含 70.26% As 和 29.74% Sb(质量分数)，砷的去除效率较高。

关键词：含砷溶液；盐酸体系；电沉积；As−Sb 合金

(Edited by Mu-lan QIN)